Identification of the conducting category of individual carbon nanotubes from Stokes and anti-Stokes Raman scattering

PingHeng Tan,* Yan Tang, and ChengYong Hu
National Laboratory for Superlattices and Microstructures, P. O. Box 912, Beijing 100083, People's Republic of China

Feng Li, YongLiang Wei, and HuiMing Cheng
Institute of Metal Research, Chinese Academy of Sciences, Shenyang 110015, People's Republic of China
(Received 17 April 2000)

Raman spectra of radial breathing modes (RBM's) of single-walled carbon nanotubes (SWNT's) are reported to exhibit a different resonantly enhanced behavior between the Stokes and anti-Stokes Raman-scattering components, from which we determine the electronic transition energy of individual SWNT's that is involved in the resonant process. By comparing the measured electronic transition energy with the theoretical energy separations between singularities in the one-dimensional density of electronic states for metallic or semiconducting SWNT's, the conducting category of observed SWNT's is identified. Moreover, we find that the relative intensity of each RBM does not reflect the proportion of a particular SWNT due to the coexistence of resonant and nonresonant Raman-scattering processes for different diametric SWNT's.

I. INTRODUCTION

Single-walled carbon nanotubes (SWNT's)[1] have attracted great attention in both experimental[2–4] and theoretical[5–8] researches because they provide an ideal model for a one-dimensional (1D) system.[9] According to theoretical calculations,[5,6] SWNT's can exhibit either metallic or semiconducting behavior depending on their diameter and chirality. This behavior has been confirmed by the scanning tunneling microscopy studies recently.[3,4] Because of their unique electrical properties and nanoscale dimensions, SWNT's are good candidates for nanoscale electronic devices.[10–12] However, nanotube production grown by almost all the known methods consists of many SWNT's with mixed, quasirandom dimensions and chiralities, and thus different electronic properties.[13–15] Therefore, it is often unknown whether the produced nanotubes are mainly metallic or mainly semiconducting. The large sample inhomogeneity makes it inconvenient to probe the main electronic properties of SWNT production by using scanning tunneling microscopy (STM) technology. Some methods such as high-resolution electron energy loss spectroscopy and optical-absorption spectroscopy[16,17] have been used to study the mean electronic properties of SWNT production, but they cannot offer the electronic properties of *individual* carbon nanotubes with the selected diameter. As a simple experimental technique that does not require difficult sample preparation techniques, Raman scattering has been used to determine the diameters of SWNT's (Ref. 18) and study the resonant process of the metallic nanotubes in a SWNT sample with small diameter dispersion.[19] However, it is very difficult to investigate the resonant Raman behavior of SWNT's when the product is very inhomogenous and has large diameter dispersion because the resonant Raman spectra are usually obtained in different experimental setups and with different laser sources.[19] In this paper, we report that the resonant behavior of individual carbon nanotubes can be investigated from the Stokes and anti-Stokes Raman-scattering spectra of their radial breathing modes, and the electronic transition energies involved in the resonant process are measured. By comparing the measured energies of electronic transitions with the theoretical results, we have identified the conducting category of individual carbon nanotubes with the diameters that are determined from the frequency of the corresponding breathing modes.

II. EXPERIMENT

SWNT samples were prepared by using an improved floating catalyst method.[20] The SWNT's have a wider diameter distribution and larger mean diameter in comparison with those obtained by the laser vaporization and electric arc techniques.[14,21] High-resolution transmission electron microscope images show that more than 75% of the SWNT's have diameters ranging from 1.0 to 2.0 nm, with a Gaussian mean diameter of 1.69 ± 0.34 nm.[20,22]

Raman scattering spectra were recorded by the Dilor SuperLabram with a typical resolution of 0.5 cm^{-1} in the measured frequency region. All spectra reported here were measured in the backscattering geometry using 632.8-nm laser excitation at the room temperature. The Raman system consists of a holographic notch filter for Rayleigh rejection and a microscope with a $100\times$ objective lens (numerical aperture $=0.9$), which allows a spatial resolution of less than 2 μm. Typically, a low-laser power of 10 kW/cm^2 was used to avoid sample heating.

III. RESULTS AND DISCUSION

Figure 1 shows the Raman spectra of SWNT's at two different sample positions excited with a He-Ne laser line (632.8 nm). The modes in the range between 100 and 300 cm^{-1} are designated as the radial breathing modes, and those in the higher-frequency region up to 500 cm^{-1} should be second-order Raman modes of the serial radial breathing modes (RBM's). For example, the overtones of strong

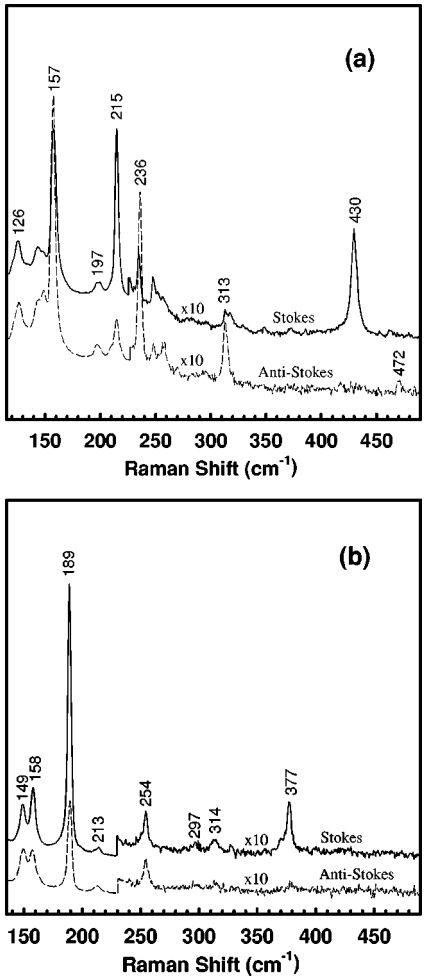

FIG. 1. The Raman-scattering spectra of radial breathing modes at different position (a) and (b) of SWNT samples. All the anti-Stokes modes have been multiplied the factor $\alpha_{s/as}$ defined in the text for comparing their resonant behavior with that of Stokes component.

RBM's located at 157, 215, and 189 cm^{-1} are observed at 313, 430, and 377 cm^{-1}, respectively. Recent calculations[18] show that the RBM frequency is related to the diameter of SWNT by a simple formula $\omega(cm^{-1})=223.75(cm^{-1}nm)/d(nm)$. From this equation, we can get the diameters of the observed nanotubes in the range of 0.9–1.8 nm, which are consistent with the diameter dispersion of our samples.[20,22]

For any mode observed in the Stokes Raman spectra, there is a corresponding mode with the same frequency at anti-Stokes side as shown in Fig. 1. It is well known that the relative intensity between Stokes and anti-Stokes lines under the nonresonant condition can be written as[23]

$$I_s=[(\omega_I-\omega)/(\omega_I+\omega)]^4[n(\omega)+1]/n(\omega)I_{as}=\alpha_{s/as}I_{as}, \tag{1}$$

where ω_I and ω are the frequencies of incident light and phonon, respectively, and $n(\omega)$ is the Bose-Einstein thermal factor

$$n(\omega)=1/[\exp(\hbar\omega/k_BT)-1], \tag{2}$$

where k_B is Boltzmann's constant and T the sample temperature. Equation (1) is usually used to estimate the sample temperature.[24] In our experiment, the sample is kept at room temperature (~300 K) because no frequency shift induced by the change of sample temperature is observed when the excitation power is much lower or little higher than the current laser density.[24] The measured anti-Stokes Raman spectra have been multiplied by a correction factor $\alpha_{s/as}$ for the room temperature, and are shown in the Fig. 1 with the x scale of the corresponding Stokes modes for the convenience to compare them with each other.

In the nonresonant case, the Raman spectra should show the symmetric profiles between the Stokes side and anti-Stokes side that has been multiplied by the factor $\alpha_{s/as}$. However, Raman spectra of RBM's in Fig. 1 show very asymmetric profiles between the Stokes and anti-Stokes sides. The intensities of Stokes and corrected anti-Stokes components of some breathing modes located at about 126, 149, 197, and 254 cm^{-1} are almost equal to each other, which behaves as the nonresonant case.[23] Whereas the intensity of the Stokes mode at 215 cm^{-1} is much stronger than that of the corresponding anti-Stokes mode, and that of the 236-cm^{-1} mode is strongly enhanced at anti-Stokes side. This different intensity between Stokes and anti-Stokes scattering components is more remarkable for the second-order modes of RBM's (e.g., 313, 377 and 430 cm^{-1}). These results indicate that many RBM's exhibit much different resonant process between the Stokes and anti-Stokes sides. For SWNT's with larger diameters, the energy separations between spikes in the 1D electronic density-of-states (DOS) are much smaller and far from the incident photon energy. Therefore, the Stokes and anti-Stokes components of those breathing modes located at about 126 and 149 cm^{-1} do not exhibit the resonant enhancement process. However, for some special diametric SWNT's, the energy separations of 1D spikes are closer to the energy of Stokes or anti-Stokes scattering photon, and hence the intensity of some breathing modes (e.g., 158-, 189- and 215-cm^{-1} modes) is much resonantly enhanced at Stokes side and other modes (e.g., 157- and 236-cm^{-1} modes) show a strong resonantly-enhanced process at anti-Stokes side. Because of the sample inhomogeneity and the diameter-selective resonant Raman effect discussed above, the Raman spectra of radial breathing modes are very sensitive to the sample position and the laser energy.[15,19] This explains why Raman spectra at two different sample positions are very different [see Fig. 1(a) and 1(b)].

The above discussions show that Raman-scattering processes for some SWNT's are under nonresonant conditions whereas the radial breathing modes of other special diametric SWNT's are resonant. Therefore, the relative intensity of each breathing mode does not reflect the proportion of a particular SWNT with the corresponding diameter. However, the comparison between Stokes and anti-Stokes Raman-scattering intensity enables us to obtain the relative proportion of the observed SWNT's with some special diameters. Because the energy difference between the Stokes and anti-Stokes sides is very small (~40 meV), the intensity of Stokes and anti-Stokes breathing modes is strongly enhanced under the resonant scattering condition. Thus, the SWNT's whose RBM's are beyond the resonance condition but their intensity is comparable to other resonant RBM's should have a larger population in the observed SWNT's.

TABLE I. Overview of electronic transition energy ($E_{experiment}$) measured in the experiment and theoretically calculated energy separations (E_{11-M}, E_{22-S}, and E_{33-S}) of the singularities of electronic states on individual SWNT's observed in the Raman spectra of Fig. 1. The value of 3100 meV for the overlap integral was used in the theoretical calculation. The accuracy of $E_{experiment}$ is mainly limited by the accuracy of sample temperature, and is less than 50 meV. Accuracy in E_{11-m} and E_{22-s} is within 10% because of the different wrapping angles, and accuracy in E_{33-s} may be much larger than that in E_{22-s}. The symbols ''*M*'' (metallic) and ''*S*'' (semiconducting) represent the conducting category of the observed SWNT's.

Frequency (cm^{-1})	126	149	157	158	189	197	213	215	236	254
Diameter (nm)	1.78	1.50	1.43	1.42	1.18	1.14	1.05	1.04	0.95	0.88
$E_{experiment}$ (meV)			2090	1840	1860			1880	2060	
E_{11-m} (meV)	1490	1760	1850	1865	2230	2330	2510	2540	2785	3000
E_{22-s} (meV)	990	1170	1235	1245	1490	1550	1675	1690	1855	2000
E_{33-s} (meV)	1980	2340	2470	2490	2980	3100	3350	3380	3710	4000
Conducting category	*M*	*S*	*M*	*M*	*M*		*M*	*S*	*S*	*M*

The electronic transitions of some SWNT's are involved in the resonant Raman process. To determine the involved electronic transitions, one must consider the relative intensity of breathing modes between the Stokes and anti-Stokes sides under the resonant condition. When the energy difference between spikes of the electronic DOS is close to the incident photon energy or the scattered photon energy, Raman scattering will exhibit the resonantly enhanced process. Under the resonant process, the Raman cross section is only determined by the electronic transition energy that is the closest to the frequency of incident or scattering photon, and the intensity of the Stokes and anti-Stokes lines is, respectively, given by[19,23]

$$I_s \propto [(E_{sampl}-E_{laser})^2+\gamma_e^2/4]^{-1} \times [(E_{sampl}-E_{laser}+E_{phonon})^2+\gamma_e^2/4]^{-1} \quad (3)$$

and

$$I_{as} \propto [(E_{sampl}-E_{laser})^2+\gamma_e^2/4]^{-1} \times [(E_{sampl}-E_{laser}-E_{phonon})^2+\gamma_e^2/4]^{-1}, \quad (4)$$

where E_{sampl} and E_{phonon}, respectively, are the energies of the electronic transition and phonon of vibrational system, and E_{laser} is the photon energy of laser. The damping factor γ_e avoids the divergence of the double-resonance expression for the Raman cross section and accounts for the width of the singularities in the electronic DOS and the lifetime of the excited state. Therefore, the relative intensity between the Stokes and anti-Stokes lines is given by

$$I_s/I_{as} = \alpha_{s/as}[(E_{sampl}-E_{laser}-E_{phonon})^2 + \gamma_e^2/4]/[(E_{sampl}-E_{laser}+E_{phonon})^2+\gamma_e^2/4]. \quad (5)$$

Because the energy shift between Stokes and anti-Stokes sides of the breathing modes is very small (~50 meV) and the same Raman modes of RBM's at two sides exhibit very different resonantly enhanced process, the width of the singularities in the electronic DOS of SWNT's is very small. When taking the damping factor γ_e as 40 meV, which is directly deduced from the scanning tunneling spectroscopy measurement,[3,4] the energies of electronic transitions ($E_{experiment}$) associated with the resonantly enhanced process of Stokes and anti-Stokes components at room temperature, can be obtained from Eq. (5), and are listed in Table I for all RBM's.

Many theoretical calculations predicted that the frequency of breathing mode is only sensitive to inverse diameter but not to the helicity (or symmetry) of a particular tube.[18] Thus, the different resonant enhancement between the Stokes and anti-Stokes components of RBM's reflects the tube diameter dependence of energy separation between the singularities of 1D electronic DOS. In the range of diameter (0.9–1.8 nm) for the observed tubes, the energies for $v_2 \rightarrow c_2$ transition in metallic tubes and $v_1 \rightarrow c_1$ transition in semiconducting tubes are much larger or smaller than the incident photon energy (1.96 eV).[7,8] The electronic transitions between the mth maximum of the valence band and the $(m \pm 1)$th minimum of the conduction band, such as $v_2 \rightarrow c_3$ and $v_2 \rightarrow c_1$, associate electronic states with different wave vectors and have smaller probability.[7,19] Therefore, for electronic transitions that are involved in the resonant Raman-scattering process, we only consider the $v_1 \rightarrow c_1$ transition of metallic tubes or the $v_2 \rightarrow c_2$ and $v_3 \rightarrow c_3$ transitions of semiconducting tubes. The theoretical calculations[7,8] showed that the diameter (d) dependence of the energy separation $E_{11}=E_{c1}-E_{v1}$ for metallic SWNT's is equal to $6\gamma_0 a_{C-C}/d$, where γ_0 is the nearest-neighbor overlap integral and a_{C-C} denotes the C-C distance. The calculated energy separations $E_{22}=E_{c2}-E_{v2}$ and $E_{33}=E_{c3}-E_{v3}$ for semiconducting SWNT's are about $4\gamma_0 a_{C-C}/d$ and $8\gamma_0 a_{C-C}/d$, respectively.[7,8] In addition, the theoretical calculation and experimental results showed that the E_{11} of metallic SWNT's and the E_{22} and E_{33} of semiconducting SWNT's have a weak dependence on the wrapping angle,[3,8] which is neglected here. If taking the nearest-neighbor overlap integral γ_0 as 3100 meV from the tight-binding approximation,[25,26] the calculated energy separation E_{11-M} between the first pair of 1D electronic DOS singularities for metallic SWNT's and those of second (E_{22-S}) and third (E_{33-S}) singularity pairs for semiconducting SWNT's are listed in Table I.

In Table I, some $E_{experiment}$ values can not be determined by Eq. (5) because the intensities of Stokes and anti-Stokes components of RBM's are equal to each other and those SWNT's are beyond the resonant condition. In other words, the energy separations of 1D electronic spikes of those SWNT's are far away from the incident photon energy. But,

the electronic transition energies of other SWNT's involved in the resonant process have been determined, and are qualitatively in accord with theoretical energy separations between 1D electronic DOS spikes of metallic or semiconducting SWNT's.[27] This accordance enables us to determine the conducting category of the observed SWNT's. For example, the oberved SWNT's with 236-cm^{-1} RBM are semiconducting because the calculated E_{22} of semiconducting SWNT's is consistent with the experimentally measured electronic transition energy. Some calculated energy separations of SWNT's with particular conducting category are close to the incident photon energy (1.96 eV), but the resonant behavior is not observed in the Raman spectra of those SWNT's. This indicates that those SWNT's do not belong to that conducting category, but the other conducting category. For instance, the observed SWNT's with nonresonant 213-cm^{-1} RBM should be the metallic category because the calculated E_{22} of semiconducting SWNT's is close to the excitation energy. Moreover, in Fig. 1 and Table I, we note that SWNT's with nearly the same diameters 1.42 and 1.43 nm (with RBM's at 158 and 157 cm^{-1}, respectively) show different resonant behavior and different electronic transition energies (a change of $\sim$250 meV). This can be regarded as an evidence that the electronic properties of SWNT's depend on the their helicity sensitively.[3]

From the above discussions, we can see that the electronic transition energy and conducting category of SWNT's can be deduced from the resonant behavior of the radial breathing mode. However, it should be pointed out that the identification of the conducting category depends on the choice of the overlap integral γ_0. The value for the overlap integral of carbon nanotubes is not yet well established. The values reported in the literature range from about 2400 to 3150 meV.[3,4,9,19,25,26,28,29] Therefore, the category identification of some observed diametric SWNT's may be different if considering a lower value for the overlap integral, such as 2500 meV. A number of experimental studies tend to take a higher value from 2900 meV to 3150 meV for the overlap integral.[19,28,29] We find that the value of 3100 meV is better fit to our experimental results, especially for the nanotubes with the RBM's that exhibit strong resonant process. When the Raman scattering of SWNT's occurs beyond the resonant condition, the electronic transition energy of those SWNT's cannot be determined from Raman spectra of the breathing modes, hence it may be impossible to determine the conducting category of those SWNT's from Raman specra excited with the used laser excitation. In this case, other laser excitation can be chosen to observe the different resonant behavior of RBM's between Stokes and anti-Stokes sides and further to identify the conducting category of those SWNT's. Although the identification of the conducting category depends on the choice of the overlap integral, it may be a feasible way to identify the conducting category of SWNT's from the Stokes and anti-Stokes Raman scattering after the precise determination of the overlap integral in the further experimental and theoretical calculations. However, the determination of the overlap integral is beyond the scope of the present paper.

IV. SUMMARY

The different resonantly enhanced Raman scattering of the radial breathing modes of SWNT's has been observed between the Stokes and anti-Stokes sides. Based on it, the electronic transition for some SWNT's that exhibit resonantly enhanced process has been determined experimentally. By comparing the measured electronic transition energy with the theoretically calculated energy separations of 1D DOS singularities of metallic or semiconducting SWNT's, the conducting category of individual carbon nanotubes is directly identified. Moreover, the results provide a strong evidence that some SWNT's are beyond the resonant condition and the Raman spectra of other special diametric SWNT's are resonant. Due to the existence of resonant and non-resonant Raman scattering processes for different diametric SWNT's, the relative intensity of each RBM does not reflect the proportion of a particular SWNT.

*Electronic mail: phtan@red.semi.ac.cn, pinghengtan@hotmail.com

[1] S. Iijima and T. Ichihashi, Nature (London) **363**, 603 (1993).
[2] A.M. Rao, E. Richter, S. Bandow, B. Chase, P.C. Eklund, K.A. Williams, S. Fang, K.R. Subbaswamy, M. Menon, A. Thess, R.E. Smalley, G. Dresselhaus, and M.S. Dresselhaus, Science **275**, 187 (1997).
[3] J.W.G. Wildöer, L.C. Venema, A.G. Rinzler, R.E. Smalley, and C. Dekker, Nature (London) **391**, 59 (1998).
[4] T.W. Odom, J.L. Huang, P. Kim, and C.M. Leiber, Nature (London) **391**, 62 (1998).
[5] J.W. Mintmire, B.I. Dunlap, and C.T. White, Phys. Rev. Lett. **68**, 631 (1992).
[6] R. Saito, M. Fujita, G. Dresselhaus, and M.S. Dresselhaus, Appl. Phys. Lett. **60**, 2204 (1992).
[7] J.C. Charlier and P. Lambin, Phys. Rev. B **57**, R15 037 (1998).
[8] C.T. White and J.W. Mintmire, Nature (London) **394**, 29 (1998).
[9] M. S. Dresselhaus, G. Dresselhaus, and P. C. Eklund, *Science of Fullerenes and Carbon Nanotubes* (Academic, San Diego, 1996).
[10] S. Saito, Science **278**, 77 (1997).
[11] S.J. Tans, M.H. Devoret, H. Dai, A. Thess, R.E. Smalley, L.J. Geerligs, and C. Dekker, Nature (London) **386**, 474 (1997).
[12] M. Bockrath, D.H. Cobden, P.L. McEuen, N.G. Ghopra, A. Zettl, A. Thess, and R.E. Smalley, Science **275**, 1922 (1997).
[13] M.S. Dresselhaus, Nature (London) **391**, 19 (1998).
[14] C. Journet, W.K. Maser, P. Bernier, A. Loiseau, M.L. de la Chapelle, S. Lefrant, P. Deniard, R. Lee, and J.E. Fischer, Nature (London) **388**, 756 (1997).
[15] M.L. de la Chapelle, S. Lefrant, C. Journet, W. Maser, P. Bernier, and A. Loiseau, Carbon **36**, 705 (1998).
[16] T. Pichler, M. Knupfer, M.S. Golden, J. Fink, A. Rinzler, and R.E. Smalley, Phys. Rev. Lett. **80**, 4729 (1998).
[17] O. Jost, A. A. Gorbunov, W. Pompe, T. Pichler, R. Friedlein, M. Knupfer, M. Reibold, H. D. Bauer, L. Dunsch, M. S. Golden, and J. Fink, Appl. Phys. Lett. **75**, 2217 (1999).
[18] S. Bandow, S. Asaka, Y. Saito, A.M. Rao, L. Grigorian, E. Richter, and P.C. Eklund, Phys. Rev. Lett. **80**, 3779 (1998).
[19] M.A. Pimenta, A. Marucci, S.A. Empedocles, M.G. Bawendi, E.B. Hanlon, A.M. Rao, P.C. Eklund, R.E. Smalley, G. Dresselhaus, and M.S. Dresselhaus, Phys. Rev. B **58**, R16 016 (1998).
[20] H.M. Cheng, F. Li, G. Su, H.Y. Pan, L.L. He, X. Sun, and M.S.

Dresselhaus, Appl. Phys. Lett. **72**, 3282 (1998).
[21] A. Thess, R. Lee, P. Nikolaev, H.J. Dai, P. Petit, J. Robert, C.H. Xu, Y.H. Lee, S.G. Kim, A.G. Rinzler, D.T. Colbert, G.E. Scuseria, D. Tomanek, J.E. Fischer, and R.E. Smalley, Science **273**, 483 (1996).
[22] P.H. Tan, Y. Tang, Y.M. Deng, F. Li, Y.L. Wei, and H.M. Cheng, Appl. Phys. Lett. **75**, 1524 (1999).
[23] W. Hayes and R. Loudon, *The Scattering of Light by Crystals* (Wiley, New York, 1976).
[24] P.H. Tan, Y.M. Deng, Q. Zhao, and W.C. Cheng, Appl. Phys. Lett. **74**, 1818 (1999).
[25] R.A. Jishi, D. Inomata, K.J. Nakao, M.S. Dresselhaus, and G. Dresselhaus, J. Phys. Soc. Jpn. **63**, 2252 (1994).
[26] J.W. Mintmire and C.T. White, Carbon **33**, 893 (1995).
[27] There exists a little difference between the theoretical calculated result and the value of electronic transition energy determined from Raman experiment. This difference results from the different chirality for given diametric SWNT's.
[28] A. Kasuya, M. Sugano, T. Maeda, Y. Saito, K. Tohji, H. Takahashi, Y. Sasaki, M. Fukushima, Y. Nishina, and C. Horie, Phys. Rev. B **57**, 4999 (1998).
[29] S.D.M. Brown, P. Corio, A. Marucci, M.A. Pimenta, M.S. Dresselhaus, and G. Dresselhaus, Phys. Rev. B **61**, 7734 (2000).